Temporal Co-Registration of Simultaneous Electromagnetic Articulography and Electroencephalography for Precise Articulatory and Neural Data Alignment

Daniel Friedrichs[1,2,3], Monica Lancheros[4], Sam Kirkham[5], Lei He[1], Andrew Clark[3], Clemens Lutz[1,3], Volker Dellwo[1,3], Steven Moran[2,6]

[1]Department of Computational Linguistics, University of Zurich, Switzerland
[2]Institute of Biology, University of Neuchâtel, Switzerland
[3]Linguistic Research Infrastructure, University of Zurich, Switzerland
[4]Faculty of Psychology and Educational Sciences, University of Geneva, Switzerland
[5]Department of Linguistics and English Language, Lancaster University, UK
[6]Department of Anthropology, University of Miami, USA
`daniel.friedrichs@uzh.ch, Monica.LancherosPompeyo@unige.ch,`
`s.kirkham@lancaster.ac.uk, lei.he@uzh.ch, andrew.clark@uzh.ch,`
`clemensfidel.lutz@uzh.ch, volker.dellwo@uzh.ch, steven.moran@unine.ch`

Abstract

This study presents a temporal co-registration method combining electromagnetic articulography (EMA) and electroencephalography (EEG) to capture the neural planning and execution phases of speech with high precision. Traditional EEG alignment based on acoustic vocal onset is often inaccurate due to the variable lag between articulatory and acoustic onsets. Our approach synchronizes EMA-derived speech kinematics with EEG data, addressing these challenges. We also examined the interaction between EMA and EEG systems, focusing on the integrity of EMA signals in the presence of EEG equipment and the electromagnetic influence of EMA on EEG signal quality. The method achieved a mean alignment delay of 2.7 ms (SD = 0.4 ms), enabling detailed analysis of pre-articulatory brain activities. Additionally, our evaluations confirmed the robustness of EMA signals and EEG event-related potentials, supporting the method's precision, feasibility, and reliability for speech planning research.

Index Terms: EMA, EEG, Co-Registration, Synchronization, Motor Speech Planning, Neural Data Alignment, Articulation

1. Introduction

Exploring the neural underpinnings of speech requires precise methods to capture the intricacies of motor planning and execution. The integration of electromagnetic articulography (EMA) and electroencephalography (EEG) offers a promising approach to speech motor control research by providing a method for synchronizing speech movement data with neural activity. This temporal co-registration is particularly useful to gain a better understanding of the timing and coordination of neural events that precede speech articulation. Prior research on speech planning has predominantly relied on the acoustic signal at vocal onset as a benchmark, which is fraught with challenges in directly pinpointing articulatory onset, as noted in several studies [1,2,3,4]. This conventional approach often falls short in accuracy, marred by the articulatory-acoustic interval (AAI), i.e., the lag between the commencement of articulatory motion and the emergence of sound [5,6]. This gap can obscure the authentic timing of speech planning and execution, potentially skewing our comprehension of speech motor planning mechanisms. Notably, the differentiation between articulatory and acoustic onsets becomes especially pronounced with voiceless stop consonants, like /t/ and /k/, where EMA's capability to detect the tongue's movement towards the alveolar ridge or velum precedes the acoustic signal significantly. EMA's refined detection contrasts sharply with acoustic analysis, which only recognizes the onset at the actual sound production after the articulatory action concludes. This distinction is pivotal since the AAI for stops may extend up to about 100 ms beyond that for non-stop phonemes [5]. Furthermore, the variability of AAIs, influenced by factors like speech rate, phonetic context, speaker's native language, dialect, and individual differences, introduces additional layers to accurately measuring speech events. The quest for greater precision in synchronizing neural data with the intricate dynamics of speech articulation has led to innovative approaches. Fargier et al. [7] pointed out the shortcomings of using acoustic energy onset for EEG data synchronization, hinting at the superior accuracy potentially offered by monitoring muscular activity. Despite this, as Van der Linden et al. [8] discovered, the complexity of speech tasks complicates the use of electromyography (EMG), due to the multiplicity of EMG bursts that can obfuscate the definitive moment of articulatory onset. Similarly, while Jouen et al. [9] suggested EEG microstates as an alternative, this method does not provide the direct measurement of articulatory movements that is possible with electromagnetic articulography (EMA). EMA's capability to precisely track speech movements at a high temporal resolution (above 1 kHz) uniquely positions it to accurately capture the onset of articulation, thereby addressing the identified gaps and providing a more reliable basis for synchronization with EEG data.

While recent advancements in magnetoencephalography (MEG) compatible systems, such as MASK (Magnetoarticulography for an Assessment of Speech Kinematics) [10,11,12], have expanded our capabilities for tracking orofacial kinematics in combination with neural data, their utility is hampered by accessibility and cost concerns. In contrast, EMA systems, particularly the Carstens AG501, have demonstrated superior accuracy and practicality for research

purposes. With a positional accuracy of up to 0.3 mm RMS, significantly outperforming MASK's up to 2 mm variability [13,14,15], and ensuring within 1 mm accuracy for head movement correction [15] (surpassing MASK's 5 mm criterion [16]), EMA systems offer unparalleled precision in articulatory onset detection.

However, integrating EMA with EEG introduces specific challenges, notably the contamination of EEG signals by muscle artifacts during overt speech production. Our study thus focuses on pre-articulatory EEG signals, which are minimally affected by these artifacts. This approach allows for a more transparent investigation into the neural underpinnings of speech planning, circumventing the distortions introduced by physical speech movements. Moreover, recent advancements in the field suggest promising methodologies for managing such interference, offering avenues for future exploration of EEG data during the entire speech production process [17,18]. In addition to muscle artifacts, electromagnetic interference from the EMA system on EEG recordings (see, for example, [19,20]) and potential distortion of EMA signals by the metal components of the EEG electrodes pose further challenges. These issues stem primarily from electromagnetic fields (EMF) generated by EMA systems, leading to noise and artifacts in EEG data through inductive or capacitive coupling. This coupling can induce currents or alter EEG setup properties, impacting recording accuracy and reliability. Even with non-ferromagnetic materials for electrodes to minimize interference, EEG's inherent electrical currents may interact with the EMA's magnetic field. These interactions may create magnetic fields around EEG wires, potentially interfering with EMA tracking and causing data distortions.

This paper presents the synchronization of the Carstens AG501 EMA and BioSemi ActiveTwo EEG systems, assessing the impact of EMA's electromagnetic field on EEG quality and the influence of EEG equipment on EMA signals. By integrating these technologies, we aim to provide a robust method for examining neural-motor coordination in speech, improving speech planning and execution analysis.

2. Methods

2.1 Apparatus and Setup

EMA data were recorded using a Carstens AG501 system (Carstens Medizinelektronik GmbH, Bovenden, Germany) featuring an array of 24 sensors for recording spatial coordinates and directional angles in three-dimensional space. The system offers high spatial resolution with approximately 0.3 mm precision and can track sensor movements at a sampling rate of up to 1250 Hz. We employed a BioSemi ActiveTwo EEG system (BioSemi BV, Amsterdam, Netherlands) equipped with 64 channels for EEG recordings, using a matching temporal resolution for EMA–EEG signal alignment.

2.2 Synchronization Procedures for EMA and EEG

To ensure precise synchronization between the EMA and EEG data, we used an Arduino Nano ESP32 microcontroller board. The device was programmed to emit a 1 ms trigger pulse to the EEG system's trigger input at both the start (T_active signal going low) and end (T_active signal going high) of each EMA data collection sweep. The effectiveness of this synchronization method was measured using an oscilloscope.

2.3 Assessing EEG Equipment's Impact on EMA Signals

We examined whether the presence and operational state of EEG equipment within the electromagnetic field could significantly affect the EMA signal characteristics. Following the method described in Kirkham et al. [21], three distinct calibration conditions were recorded three times (i.e., a total of nine sessions with three sets of 24 sensors) and compared: (1) without EEG equipment in the electromagnetic field, (2) with EEG equipment inactive (off), and (3) with EEG equipment active (on). For each calibration session (1–3), the same 24 sensors were mounted once on a circular disk (referred to as 'circal'), which was then subjected to a series of predetermined rotations, which allowed for the comparison of theoretical and actual sensor positions. Secured in magazines corresponding to designated channels, positional data, and signal strength measurements were recorded using Carsten's calibration software Cs5cal. The sensor measurements consisted of spatial coordinates (x, y, z), directional angles (phi, theta), and the root mean square (RMS) differences between expected and measured transmitter amplitudes. During the calibration procedure, sensor movements in each condition were recorded for approximately five minutes and forty-nine seconds.

2.4 Evaluating EMA Interference in EEG Signals

To evaluate the impact of EMA system interference on EEG signal quality, we conducted a two-phase experiment, with all EEG data recorded at a sampling frequency of 2048 Hz. Initially, we measured baseline noise levels by submerging an EEG cap and electrodes in a water bucket positioned beneath the EMA system, replicating the electrical properties of the human head but without the biological signals. This setup allowed for a clear assessment of EMA-induced noise on EEG recordings by comparing conditions with the EMA system's magnetic field turned off and then on, thus establishing a controlled baseline for electromagnetic interference. Subsequently, we examined the real-world implications of this interference by recording EEG data from a 30-year-old female participant. The participant was instructed to produce 180 trisyllabic sequences at a normal speech rate (e.g., /tatata/ and /takupi/) displayed on a computer screen. These recordings were conducted under identical conditions to the initial test – both with the EMA system's magnetic field inactive (serving as a control) and active – to directly assess the EMA's influence on the integrity of EEG signals in a practical speech production context.

2.5 EMA Data Analysis

To determine if the presence and operational state of the EEG equipment within the electromagnetic field could significantly affect the EMA signal characteristics, we computed two metrics. These include (1) the peak-to-peak variation (Δ), which corresponds to the difference between the minimum and maximum z-coordinate for each channel during calibration sessions, and (2) the standard deviation (σ) of the latter measure. Lower figures for both Δ and σ indicate higher calibration accuracy, with a standard deviation threshold not exceeding 0.25 mm, which is recommended for accurate calibration [13,21]. For each of these metrics, we conducted a Bayesian mixed-effects model to compare the condition without EEG recordings to the condition with the EEG system inactive and with the EEG system active, respectively. The models had random intercepts and random slopes for the

contrasts involving condition. Set was included as a covariate, but we do not report the results for this variable. The following priors were used for Δ_z and σ_z, respectively: $N(0.5,0.25)$ / $N(0.15,0.1)$ for the intercept and $N(0,0.5)$ / $N(0,0.1)$ for differences between conditions. Bayes Factors were computed for each contrast using these and more constraining priors.

A 3D visualization of sensor coil trajectories in each condition is displayed in Fig. 1.
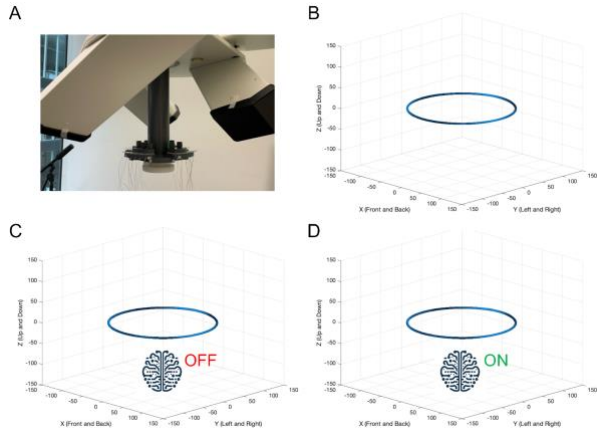

Figure 1: *EMA sensor calibration and measured trajectories for all 24 sensors of the Carstens AG501 under varying conditions. A: Standard calibration setup with sensors on a rotating 'circal' disk. B: Baseline calibration without EEG interference. C: With EEG equipment inactive (off) in the electromagnetic field. D: With EEG equipment active (on) in the electromagnetic field.*

2.6 EEG Data Analysis

For the analysis of baseline noise data collected during the first experimental phase, we performed an advanced frequency analysis. This procedure involved surveying the EEG frequency spectrum from 0 to 1024 Hz, in increments of 200 Hz. Cluster-mass statistics via permutation methods for repeated measures ANOVA were employed to scrutinize any differences in the EEG signal with the EMA system turned on and off. This analysis was conducted using the permuco4brain R package [22]. For the analysis of data obtained from the second experimental phase involving a human participant, the Cartool Software [23] was utilized for post-acquisition analysis. An initial frequency analysis of the unfiltered EEG signal, recorded over a duration of 10 seconds with a high cut-off at 130 Hz and without a notch filter, disclosed no frequency discrepancies between the EMA system being active and inactive. This finding aligns with our expectations, considering the oscillations of the magnetic field generated by the EMA system occur between 9 and 16 kHz – frequencies well beyond the EEG's typical operational range below 50 Hz [23]. Stimulus-aligned epochs – focusing on the time windows preceding articulation, from the presentation of the stimulus to about 700 ms – were extracted and band-pass filtered between 0.1 Hz and 30 Hz. A notch filter at 50 Hz was also applied. Employing a fixed 700-ms window for EEG analysis, rather than aligning with the variable timing of articulatory onset, provided a controlled framework essential for more accurately assessing the impact of the EMA's magnetic field on EEG signal integrity. Epochs were visually checked and accepted only in the absence of artifacts, i.e., eyeblinks, motor artifacts, or significant amplitude variations. Accepted epochs were recalculated

against the average reference. To determine if there were differences in the electrical signal coming from the brain between EMA being active and inactive, analyses of amplitude and topography of our interest were carried out. Since only one subject was recorded with EEG, both analyses of amplitude and topography were made on single-trial event-related potentials (ERPs) (65 epochs per condition) instead of one participant's averaged ERPs. Single-trial methods have been proven to be reliable and effective since they preserve the variability of the EEG dataset.

3. Results

3.1 Temporal Alignment and Synchronization Accuracy

Measurements of the alignment and synchronization between the EMA and EEG data streams revealed high precision. An average delay of 2.7 ms with a standard deviation (SD) of 0.4 ms was measured between the T_active signal going low and the trigger pulse being sent to the EEG. Precision in this context is reflected by the SD. The smaller the SD (relative to the mean delay), the more precise the synchronization between the EMA and EEG signals

3.2 Effects of EEG Equipment on EMA Signal Integrity

Table 1 shows the mean and standard deviation for each metric across conditions. As can be seen, the figures are highly similar across conditions. The results of the statistical models are presented in Table 2. Estimates are similar across conditions, and the 95 % credible intervals for the comparisons of interest all include zero. Bayes Factors for Δ_z are all below 0.3. They provide moderate to strong evidence in favor of the hypothesis that there are no differences between conditions. Bayes Factors for σ_z are about 0.04, providing evidence in favor of the null hypothesis.

Table 1: *Mean values and standard deviations (SD) for peak-to-peak variation (Δ_z) and standard deviation of z-coordinates (σ_z) across calibration sessions under three conditions: No EEG equipment, EEG equipment inactive, and EEG equipment active in the EMA field. Data are presented as* mean (SD) *values across 24 sensors from three separate runs per condition.*

Condition	Δ_z (*SD*)	σ_z (*SD*)
No EEG	0.562 (0.090)	0.137 (0.029)
With inactive EEG	0.562 (0.090)	0.139 (0.030)
With active EEG	0.565 (0.086)	0.138 (0.030)

Table 2: *Results of the mixed-effects model for Δ_z and σ_z (estimates and 95 % credible intervals). Sliding contrasts were used such that the intercept represents the grand mean, the first estimate for Condition the difference between inactive EEG and no EEG, and the second estimate the difference between active EEG and no EEG.*

Δ_z	β	Cr.Int
Intercept	0.58	[0.550 , 0.610]
Inactive vs. no EEG	0.0001	[-0.024 , 0.024]
Active vs. no EEG	0.003	[-0.021 , 0.027]

σ_z	β	Cr.Int
Intercept	0.14	[0.13 , 0.15]
Inactive vs. no EEG	-0.0019	[-0.0096 , 0.0061]
Active vs. no EEG	0.0018	[0.0062 , 0.0099]

3.3 Impact of EMA on EEG Signal Quality

Our initial phase analysis employing comprehensive cluster-mass statistics found no significant differences in EEG signal characteristics when comparing the EMA system's active and inactive states across the tested frequency spectrum (0 to 1024 Hz, $p > 0.05$). This result was confirmed using the cluster mass method and the threshold-free cluster enhancement (TFCE) statistic [24], indicating no discernible interference from the EMA's magnetic field within the evaluated frequency range. In the participant-based phase, point-wise ERP waveform analysis revealed only one left frontal electrode showing significant differences in amplitude ($p < 0.01$) within a time window from 10 to 46 ms post-stimulus (see Fig. 2 A).
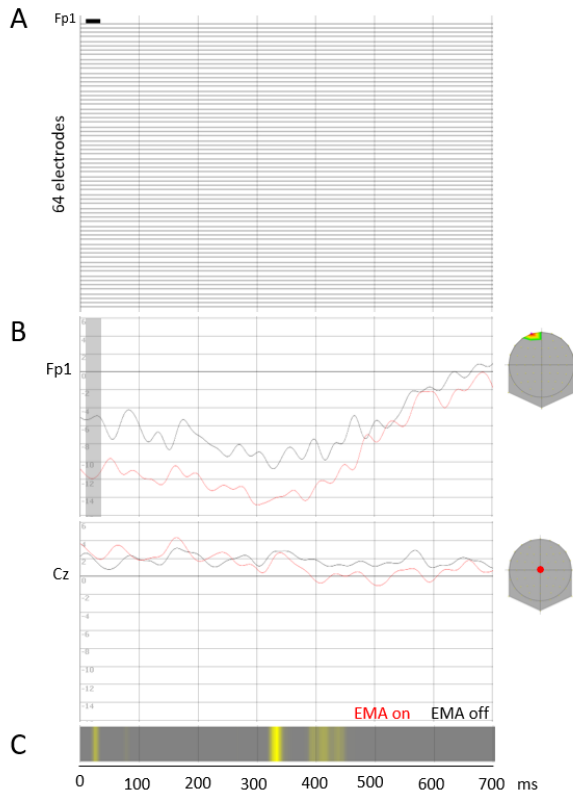

Figure 2: *Waveform and topographic analysis of EMA influence on EEG signals. A: Results of waveform analyses across all time points and electrodes, where darker areas represent significant amplitude differences (p < 0.01) when EMA is active (on) versus inactive (off). B: Sample waveforms from Fp1 and Cz electrodes, with time windows marked to show periods of statistically significant amplitude variation (p < 0.01) between active and inactive EMA states. C: Results from Topographic Analysis of Variance (TANOVA), illustrating significant differences in spatial EEG patterns (p < 0.05) between states of EMA activation. Areas of topographic dissimilarity are indicated in deeper yellow.*

Differences in amplitude on the mentioned electrode could be due to signal artifacts that might have required interpolation (not performed here). The remaining electrodes did not reveal differences in the ERP amplitudes in the analyzed time window – from the stimulus to 700 ms. Concerning the topographies, the topographic analysis of variance (TANOVA, [25]) comparing the global dissimilarity between EMA being active

and inactive revealed a relatively brief time window (from 324 to 338 ms) in which the ERPs map topographies differed ($p < 0.05$; see Fig. 2 C). However, in this kind of analysis, a time-period criterion of at least 20 ms is generally considered since topographical differences across conditions could be due to a transitional topography changing from one spatial configuration to another [2]. Therefore, applying a temporal criterion of 20 ms in this context would lead us to conclude that no discernible topographic differences exist between states of EMA activation. Taken together, results on the ERP amplitudes and topographies show that the magnetic field generated by the EMA does not cause an interference in those particular analyses.

4. Discussion

This study introduces a precise method for synchronizing EMA and EEG, significantly enhancing the temporal co-registration of articulatory and neural data in speech motor planning research. Our technique addresses the variability in the AAI, a major challenge in traditional EEG alignment with vocal onset that can obscure speech planning and execution timing. Notably, we achieved unprecedented synchronization precision, aligning EMA and EEG signals with an average delay of 2.7 ms and a standard deviation of 0.4 ms. This level of precision, essential for analyzing the variation in AAI across phonemes and other factors, allows for a more nuanced examination of neural planning and articulatory dynamics. The methodological advancements presented here mitigate previous inaccuracies encountered with acoustic cue-based methodologies, providing direct measurements of articulatory movement and neural activity with minimal interference. The demonstrated robustness of EMA signals and unaffected EEG event-related potentials, even amidst EMA's electromagnetic field, underline the reliability of our co-registration technique. Consequently, this research not only validates EMA-EEG co-registration for studying the intricate relationship between neural planning and speech execution but also sets the stage for further investigative paths.

In clinical applications, although this study does not explore specific interventions, the enhanced precision in synchronizing articulatory and neural data could inform the development of diagnostic tools and therapeutic strategies for speech disorders. Accurate temporal co-registration may improve our understanding of neural deviations in speech pathologies, guiding targeted rehabilitation techniques. Future clinical research is needed to translate these advancements into practical tools and interventions. Integrating this approach in scenarios involving overt speech and managing motion artifacts in EEG signals remains challenging and will require innovative solutions to extend the methodology, providing deeper insights into neural planning and motor execution during active speech tasks.

In summary, this study offers a new toolkit for articulatory and neural data synchronization, achieving remarkable precision and reliability in temporal co-registration. These findings not only enhance the accuracy of speech motor planning research but also encourage further exploration of the complex neural mechanisms underlying speech articulation. Future research should aim to apply these techniques in more dynamic speech scenarios to fully understand the implications of our methodology for speech science and potential clinical applications.

5. Acknowledgements

6. References

[1] M. Lancheros, A. L. Jouen, and M. Laganaro, "Neural dynamics of speech and non-speech motor planning," *Brain and Language*, vol. 203, p. 104742, 2020.

[2] R. Fargier and M. Laganaro, "Spatio-temporal dynamics of referential and inferential naming: Different brain and cognitive operations to lexical selection," *Brain Topography*, vol. 30, pp. 182-197, 2017.

[3] A. Bürki, P. P. Cheneval, and M. Laganaro, "Do speakers have access to a mental syllabary? ERP comparison of high frequency and novel syllable production," *Brain and Language*, vol. 150, pp. 90-102, 2015.

[4] M. Laganaro, "ERP topographic analyses from concept to articulation in word production studies," *Frontiers in Psychology*, vol. 5, p. 493, 2014.

[5] A. H. Kawamoto, Q. Liu, K. Mura, and A. Sanchez, "Articulatory preparation in the delayed naming task," *Journal of Memory and Language*, vol. 58, no. 2, pp. 347-365, 2008.

[6] K. Rastle, K. P. Croot, J. M. Harrington, and M. Coltheart, "Characterizing the motor execution stage of speech production: consonantal effects on delayed naming latency and onset duration," *Journal of Experimental Psychology: Human Perception and Performance*, vol. 31, no. 5, p. 1083, 2005.

[7] R. Fargier, A. Bürki, S. Pinet, F. X. Alario, and M. Laganaro, "Word onset phonetic properties and motor artifacts in speech production EEG recordings," *Psychophysiology*, vol. 55, no. 2, p. e12982, 2018.

[8] L. Van Der Linden, S. K. Riès, T. Legou, B. Burle, N. Malfait, and F. X. Alario, "A comparison of two procedures for verbal response time fractionation," *Frontiers in Psychology*, vol. 5, p. 1213, 2014.

[9] A. L. Jouen, M. Lancheros, and M. Laganaro, "Microstate ERP analyses to pinpoint the articulatory onset in speech production," *Brain Topography*, vol. 34, pp. 29-40, 2021.

[10] N. Alves, C. Jobst, F. Hotze, P. Ferrari, M. Lalancette, T. Chau, P. van Lieshout, and D. Cheyne, "An MEG-compatible electromagnetic-tracking system for monitoring orofacial kinematics," *IEEE Transactions on Biomedical Engineering*, vol. 63, no. 8, pp. 1709-1717, 2016.

[11] C. Lau, "Validation of the Magneto-Articulography for the Assessment of Speech Kinematics (MASK) System and Testing for Use in a Clinical Research Setting," Doctoral dissertation, University of Toronto, 2013.

[12] D. Cheyne, "Development of an MEG-compatible Articulography System for the Assessment of Brain Function and Oromotor Dynamics," CHRP Application – Detailed Description, pp. 1-11, 2009.

[13] Carstens Medizinelektronik GmbH, "Articulograph AG501," Available at: http://www.articulograph.de/, 2024.

[14] F. Sigona, M. Stella, A. Stella, P. Bernardini, B. G. Fivela, and M. Grimaldi, "Assessing the position tracking reliability of Carstens' AG500 and AG501 electromagnetic articulographs during constrained movements and speech tasks," *Speech Communication*, vol. 104, pp. 73-88, 2018.

[15] I. Anastasopoulou, P. van Lieshout, D. O. Cheyne, and B. W. Johnson, "Speech Kinematics and Coordination Measured With an MEG-Compatible Speech Tracking System," *Frontiers in Neurology*, vol. 13, p. 828237, 2022.

[16] M. F. Lezcano, F. Dias, A. Arias, and R. Fuentes, "Accuracy and reliability of AG501 articulograph for mandibular movement analysis: a quantitative descriptive study," *Sensors*, vol. 20, no. 21, p. 6324, 2020.

[17] G. Ouyang, W. Sommer, C. Zhou, S. Aristei, T. Pinkpank, and R. Abdel Rahman, "Articulation artifacts during overt language production in event-related brain potentials: Description and correction," *Brain Topography*, vol. 29, pp. 791-813, 2016.

[18] L. Y. Ganushchak, I. K. Christoffels, and N. O. Schiller, "The use of electroencephalography in language production research: A review," *Frontiers in Psychology*, vol. 2, p. 208, 2011.

[19] C. M. Cook, A. W. Thomas, and F. S. Prato, "Resting EEG is affected by exposure to a pulsed ELF magnetic field," *Bioelectromagnetics: Journal of the Bioelectromagnetics Society, The Society for Physical Regulation in Biology and Medicine, The European Bioelectromagnetics Association*, vol. 25, no. 3, pp. 196-203, 2004.

[20] A. V. Kramarenko and U. Tan, "Effects of high-frequency electromagnetic fields on human EEG: a brain mapping study," *International Journal of Neuroscience*, vol. 113, no. 7, pp. 1007-1019, 2003.

[21] S. Kirkham, P. Strycharczuk, E. Gorman, T. Nagamine, and A. Wrench, "Co-registration of simultaneous high speed ultrasound and electromagnetic articulography for speech production research," in *Proc. 20th Int. Congr. Phonetic Sci.*, Apr. 2023.

[22] J. Frossard and O. Renaud, "The cluster depth tests: Toward point-wise strong control of the family-wise error rate in massively univariate tests with application to M/EEG," *NeuroImage*, vol. 247, p. 118824, 2022.

[23] D. Brunet, M. M. Murray, and C. M. Michel, "Spatiotemporal analysis of multichannel EEG: CARTOOL," *Computational Intelligence and Neuroscience*, vol. 2011, pp. 1-15, 2011.

[24] S. M. Smith and T. E. Nichols, "Threshold-free cluster enhancement: addressing problems of smoothing, threshold dependence and localisation in cluster inference," *NeuroImage*, vol. 44, no. 1, pp. 83-98, 2009.

[25] M. M. Murray, D. Brunet, and C. M. Michel, "Topographic ERP analyses: A step-by-step tutorial review," *Brain Topography*, vol. 20, no. 4, pp. 249-264, 2008.